Prospective Study of Serial ^{18}F-FDG PET and ^{18}F-Fluoride PET to Predict Time to Skeletal-Related Events, Time to Progression, and Survival in Patients with Bone-Dominant Metastatic Breast Cancer

Lanell M. Peterson[1], Janet O'Sullivan[2], Qian (Vicky) Wu[3], Alena Novakova-Jiresova[1], Isaac Jenkins[3], Jean H. Lee[4], Andrew Shields[4], Susan Montgomery[5], Hannah M. Linden[1,3], Julie Gralow[1,3], Vijayakrishna K. Gadi[1,3], Mark Muzi[4], Paul Kinahan[4], David Mankoff[6], and Jennifer M. Specht[1,3]

[1]Division of Medical Oncology, University of Washington, Seattle, Washington; [2]Department of Statistics, University College Cork, Cork, Ireland; [3]Clinical Research Division, Fred Hutchinson Cancer Research Center, Seattle, Washington; [4]Department of Radiology, University of Washington, Seattle, Washington; [5]Swedish Cancer Institute, Edmonds, Washington; and [6]Department of Radiology, University of Pennsylvania, Philadelphia, Pennsylvania

Assessing therapy response of breast cancer bone metastases is challenging. In retrospective studies, serial ^{18}F-FDG PET was predictive of time to skeletal-related events (tSRE) and time to progression (TTP). ^{18}F-NaF PET improves bone metastasis detection compared with bone scanning. We prospectively tested ^{18}F-FDG PET and ^{18}F-NaF PET to predict tSRE, TTP, and overall survival (OS) in patients with bone-dominant metastatic breast cancer (MBC). **Methods:** Patients with bone-dominant MBC were imaged with ^{18}F-FDG PET and ^{18}F-NaF PET before starting new therapy (scan1) and again at a range of times centered around approximately 4 mo later (scan2). Maximum standardized uptake value (SUV_{max}) and lean body mass adjusted standardized uptake (SUL_{peak}) were recorded for a single index lesion and up to 5 most dominant lesions for each scan. tSRE, TTP, and OS were assessed exclusive of the PET images. Univariate Cox regression was performed to test the association between clinical endpoints and ^{18}F-FDG PET and ^{18}F-NaF PET measures. mPERCIST (Modified PET Response Criteria in Solid Tumors) were also applied. Survival curves for mPERCIST compared response categories of complete response+partial response+stable disease versus progressive disease for tSRE, TTP, and OS. **Results:** Twenty-eight patients were evaluated. Higher ^{18}F-FDG SUL_{peak} at scan2 predicted shorter time to tSRE ($P = <0.001$) and TTP ($P = 0.044$). Higher ^{18}F-FDG SUV_{max} at scan2 predicted a shorter time to tSRE ($P = <0.001$). A multivariable model using ^{18}F-FDG SUV_{max} of the index lesion at scan1 plus the difference in SUV_{max} of up to 5 lesions between scans was predictive for tSRE and TTP. Among 24 patients evaluable by ^{18}F-FDG PET mPERCIST, tSRE and TTP were longer in responders (complete response, partial response, or stable disease) than in nonresponders (progressive disease) ($P = 0.007$, 0.028, respectively), with a trend toward improved survival ($P = 0.1$). An increase in the uptake between scans of up to 5 lesions by ^{18}F-NaF PET was associated with longer OS ($P = 0.027$). **Conclusion:** Changes in ^{18}F-FDG PET parameters during therapy are predictive of tSRE and TTP, but not OS. mPERCIST evaluation in bone lesions may be useful in assessing response to therapy and is worthy of evaluation in multicenter, prospective trials. Serial ^{18}F-NaF PET was associated with OS but was not useful for predicting TTP or tSRE in bone-dominant MBC.

Key Words: ^{18}F-FDG PET; ^{18}F-NaF PET; bone dominant breast cancer; response to therapy

J Nucl Med 2018; 59:1823–1830
DOI: 10.2967/jnumed.118.211102

Bone is the most common site of breast cancer metastases (*1–3*) and is associated with significant morbidity (*4*). Patients with bone-dominant (BD) disease (involving exclusively bone or bone and soft tissue without visceral organ involvement) experience longer survival than those patients with predominantly visceral metastases (*5–10*). Bone metastases are detected using a variety of imaging modalities (*11*). However, assessing response to therapy in patients with BD metastatic breast cancer (MBC) remains challenging. Bone scans visualize the response of surrounding bone to cancer and may be slow to show response, and may even show a "flare" related to bone healing with effective therapy. Similar findings may occur with other modalities including CT (*12–15*). RECIST 1.1 specifically excludes bone metastasis as a measurable site for response, and BD MBC patients are often excluded from clinical trials that measure response (*4,16–19*). This represents a large patient population that could benefit from improved use of systemic therapy, making accurate assessment of BD MBC response an imperative need.

^{18}F-FDG PET depicts aspects of breast cancer bone metastases distinct from bone scans, ^{18}F-NaF PET, and other modalities and may therefore offer a superior approach for assessing response for BD MBC patients (*11*). ^{18}F-FDG PET is hypothesized to visualize tumor metabolism (*11*). Compared with bone scans and ^{18}F-NaF PET, ^{18}F-FDG has higher uptake in more lytic bone metastases, making ^{18}F-FDG PET more sensitive for these lesions, whereas bone scanning and ^{18}F-NaF PET perform better in identifying more blastic metastases (*20–22*). Although cases of flare in response to therapy have been reported on ^{18}F-FDG PET (*23*), this appears to be a rare event (*24*), and largely related to the known impact of agonist endocrine agents

Received Mar. 14, 2018; revision accepted Apr. 30, 2018.
For correspondence or reprints contact: Lanell M. Peterson, 825 Eastlake Ave., E. Valley Building LV-200, Seattle, WA 98101.
E-mail: lanell@uw.edu
Published online May 10, 2018.

(*25*). Previously reported retrospective data show that serial ^{18}F-FDG PET can be used to measure bone metastasis response to therapy and to predict outcome (*26–29*). Higher ^{18}F-FDG uptake predicted the time to skeletal-related event (tSRE) and changes in ^{18}F-FDG uptake with treatment predicted time-to-progression (TTP). Alternatively, ^{18}F-NaF PET offers improved resolution and quantitative capability compared with bone scanning and bone SPECT (*22,30–33*) and might therefore offer benefit for assessing response and progression, as reported for prostate cancer (*34*). We therefore evaluated both serial ^{18}F-NaF PET and ^{18}F-FDG PET to predict tSRE, TTP, and overall survival (OS) in a prospective study of patients with BD MBC starting new systemic therapy.

MATERIALS AND METHODS

Patient Eligibility

Eligible patients had histologically confirmed breast cancer, imaging findings of bone metastases, and no contraindications to PET imaging. The institutional review board approved this study, and all patients signed a written informed consent form and agreed to undergo 4 PET scans (2 ^{18}F-FDG PET and 2 ^{18}F-NaF PET), as well as standard pretherapy and clinical follow-up to determine response to therapy. Baseline ^{18}F-FDG PET and ^{18}F-NaF PET scans (scan1) were completed before initiation of new systemic therapy. Follow-up ^{18}F-FDG PET and ^{18}F-NaF PET scans (scan2) were completed at the discretion of the treating physician. The date of the ^{18}F-NaF PET scan1 was used to indicate the date of study entry. Full selection criteria are provided in Supplemental Table 1 (supplemental materials are available at http://jnm.snmjournals.org).

PET Imaging

^{18}F-FDG and ^{18}F-NaF were produced at the University of Washington Cyclotron facility or purchased from commercial suppliers (Cardinal Health) in accord with manufacturing requirements for both tracer (*35,36*). ^{18}F-FDG imaging was performed according to routine clinical protocol (*37*) on 1 of 3 institutional tomographs (Advance PET and 2 DSTE PET/CT scanners; GE Healthcare). Fasting was not required for ^{18}F-NaF PET studies, and patients underwent a 60-min dynamic scan before the torso survey. Scanners were calibrated using the manufacturer's recommended procedures and cross-calibrated regularly for quantitative comparisons (*38,39*). Most patients were imaged on the same scanner in serial studies for each tracer; however, because of the addition of a second GE Discovery STE PET/CT at our center, some patients underwent scan2 on the alternate scanner. We have shown that our calibration and cross-calibration procedures and identical acquisition and reconstruction protocols provide test–retest accuracy comparable to a well-calibrated single scanner (*40*).

Image Analysis

Experienced nuclear medicine physicians reviewed the ^{18}F-FDG PET and ^{18}F-NaF PET scans (as well as corresponding CTs) to identify the same bone lesions on both scans (up to 10 lesions), including the 5 most dominant, not previously irradiated, for each scan. Dominant lesions were selected on the basis of tracer uptake, not lesion size. The index lesion was defined as the lesion with the largest amount of tracer uptake in each scan, and was not necessarily the same lesion in both scans. In the ^{18}F-NaF PET scan, for each identified lesion and corresponding normal bone, square (3 × 3 pixel, ~1 cm) regions-of-interest (ROIs) were drawn on 3 adjacent planes where the pixel of maximum value was included in each lesion ROI. For the ^{18}F-FDG PET scans, ROIs for tumor and liver were drawn according to PERCIST (*41,42*).

Cancer Therapy and Determination of Response Endpoints

Systemic therapy for MBC was selected by the treating physician before baseline scans. Outcome data were ascertained from prospectively collected clinical data. tSRE was defined as time from study entry to pathologic fracture, need for radiation to stabilize bone lesion, or hypercalcemia of malignancy. TTP and OS were defined as time from study entry to disease progression or death. tSRE and TTP were adjudicated by medical oncology review of clinical data independent of PET scan results obtained during trial participation. Supplemental Table 2 details the PET imaging metrics, including standardized uptake value (SUV) and lean body mass adjusted standardized uptake (SUL), and their formulation.

mPERCIST Evaluation

On the basis of our preliminary analysis, bone lesions have lower average SUL_{peak} values than soft-tissue lesions previously studied using PERCIST (*41,42*). Thus, our mPERCIST (Modified PET Response Criteria in Solid Tumors) lesion inclusion criteria included bone lesions with an SUL_{peak} greater than 1.5× mean liver SUL, instead of 1.5× mean liver SUL + 2 SDs of the mean liver SUL. For the patients meeting this requirement, we followed the published PERCIST metabolic response criteria and classified patients as mPERCIST responders (complete response [CR], partial response [PR], or stable disease) or nonresponders (progressive disease [PD]).

Statistical Analysis

Univariate Cox proportional hazards regression models for each of the clinical endpoints (tSRE, TTP, OS) were performed for each of the SUV measures of interest. ^{18}F-FDG PET variables showing promise in the univariate analysis were included in a multivariable Cox model (*43*). Hazard ratios, P values for the regression coefficients, R^2, and index of concordance are reported. The primary objective (and preplanned analysis) was to determine whether SUV_{max} from bone metastases were useful prognostic indicators for progression and SREs. We considered multiple tests that included SUV_{max} at both scan1 and scan2, along with a mean of all available sites at scan1 and scan2. Other tests were considered for several other prognostic factors and secondary endpoints, as well as for other definitions of SUV. If this were a definitive clinical trial, the Bonferroni procedure (or other multiple testing procedure) should be applied in all instances in which multiple testing occurs. However, the scope of this study is more limited. The results presented provide an indication of directions for future validation in a rigorously conducted prospective clinical trial. We report standard P values but include a clear caveat detailing limitations of the study and its exploratory nature.

To test the association between mPERCIST response criteria (discrete variables) and clinical endpoints, Kaplan–Meier curves for patients in mPERCIST response profiles (CR+PR+stable disease vs. PD) were evaluated for each endpoint and quantitatively assessed using the log-rank test.

RESULTS

Twenty-eight patients are included in this study. Twenty-four patients completed all scans (2 ^{18}F-NaF PET and 2 ^{18}F-FDG PET) and an additional 4 patients completed paired ^{18}F-FDG PET, but not paired ^{18}F-NaF PET scans. Trial accrual fell short of goal, but was stopped due to financial and logistical challenges, and not based on interim data analysis. Ten patients had their second scan obtained on a different scanner within the same institution (6 on the same model DSTE). Table 1 summarizes the patient and tumor characteristics, which were taken from metastatic biopsy (if available) or from breast primary. Most had hormone receptor–positive, human epidermal growth factor receptor 2–negative disease. The average number of prior therapies for MBC was 2.7 (range, 0–8). Most patients (61%) started a new endocrine therapy after scan1. Twenty patients received bisphosphonates, and 2 patients received an anti-RANK ligand agent. No patient changed bone-stabilizing agents while on the study. Although more than 100 lesions were identified

TABLE 1
Selected Patient and Tumor Characteristics

Characteristic	$n = 28$ (%)	Mean (range)
Age (y)		56 (33–90)
Histology		
Ductal	18 (64%)	
Lobular	4 (14%)	
Mixed or unknown	6 (21%)	
Receptor status		
Estrogen receptor–positive	24 (86%)	
Progesterone receptor–positive	21 (75%)	
Human epidermal growth factor receptor 2–negative	20 (70%)	
Dominant lesion type		
Lytic	11 (39%)	
Sclerotic	7 (25%)	
Mixed	8 (29%)	
Unknown	2 (7%)	
Bone lesions per patient		
1–5	11 (39%)	
6–10	3 (11%)	
>10	14 (50%)	
Prior therapy		
Chemotherapy	15 (54%)	
Endocrine therapy	17 (61%)	
Radiation	13 (46%)	
No. of prior therapies before enrollment		2.7 (0–8)
On study therapy*		
Chemotherapy	11 (39%)	
Endocrine therapy	17 (61%)	
Time from diagnosis to metastatic diagnosis		71.8 mo (0–440.3)
Time from metastatic diagnosis to enrollment		18.3 mo (0–71.4)

*Biologic therapy (trastuzumab) was given with chemotherapy or endocrine therapy for patients with human epidermal growth factor receptor 2–positive disease.

among the patients, the focus of this analysis was on the index lesion and 5 most dominant lesions in each scan. Disease burden assessed by number of lesions per patient is shown in Table 1.

Response measures for all patients are included in Supplemental Table 3. Figure 1 illustrates an example of PR by ^{18}F-FDG PET with stable NaF uptake in bone metastases. Over half of the patients had an SRE, with the median time of 8.3 mo (0.0–86.5 mo). Median TTP was 5.8 mo (2.2–29.5 mo). All but 3 patients died, with a median survival of 35.0 mo by Kaplan–Meier estimate, (6.06–87.29 mo).

Supplemental Table 4 summarizes the interval between initial (scan1) and follow-up (scan2), which was determined by the treating physician and therefore varied (mean, 4.3 mo). Descriptive statistics for the index lesion and multiple lesion uptake measures are shown in Table 2, and univariate analysis of ^{18}F-FDG PET and ^{18}F-NaF PET measures to clinical endpoints (tSRE, TTP, and OS) are shown in Table 3. Persistence of ^{18}F-FDG uptake (SUV_{max}) in the index lesion at scan2 was associated with shorter tSRE (hazard ratio [HR], 2.27; $P < 0.001$). Persistence of ^{18}F-FDG–avid disease at scan2 by SUL_{peak} was associated with shorter time to SRE (HR, 2.41; $P < 0.001$) and shorter TTP (HR, 1.58; $P = 0.044$). SUL_{peak} unit difference for up to 5 lesions between scan1 and 2 was also associated with shorter time to SRE (HR, 2.21; $P = 0.038$). ^{18}F-FDG SUV_{max} at scan1 was not predictive of tSRE, TTP, or OS. Persistence of ^{18}F-FDG at scan2 by SUV_{max} or SUL_{peak} of index lesion or lesser change in mean SUL_{peak} of up to 5 lesions were predictive of shorter time to SRE or TTP, but none was associated with OS.

For ^{18}F-NaF PET, an increase in the percentage change of the mean SUV_{max} of up to 5 lesions was associated with longer OS ($P = 0.027$). This association did not persist when SUV uptake was corrected for normal bone uptake ($P = 0.237$) (Supplemental Table 5). No other associations between NaF PET parameters at scan1 or scan2 or change between scans and clinical outcomes were observed. Analyses of ^{18}F-FDG PET and ^{18}F-NaF PET measures by type of therapy (endocrine or chemotherapy), time between scans, and primary lesion type (lytic or sclerotic) are shown in Supplemental Table 6. We found no significant difference in performance of ^{18}F-FDG PET or ^{18}F-NaF PET in these subgroups.

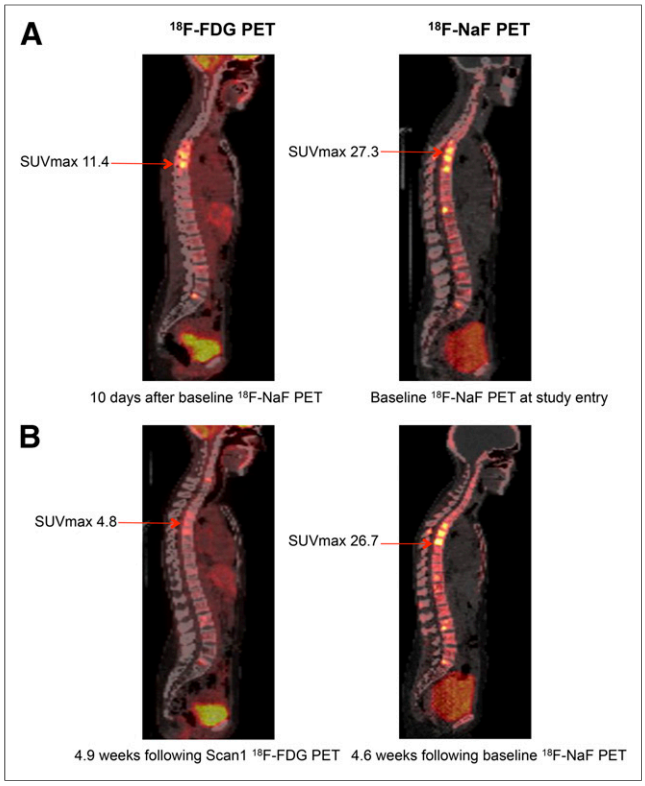

FIGURE 1. Sagittal images of a 43-y-old woman: scan1 (A) and scan2 (B). Index lesions (not same lesions) decreased 58% by ^{18}F-FDG PET and 2% by ^{18}F-NaF PET. Response was considered partial by mPERCIST. Bone metastases were considered stable by ^{18}F-NaF PET.

Univariate analysis failed to support ^{18}F-NaF PET imaging as a useful predictor of tSRE and TTP; therefore, subsequent multivariable analysis included ^{18}F-FDG PET parameters (Table 4). A model incorporating SUV_{max} of the index lesion at scan1 and unit difference in SUV_{max} in up to 5 lesions led to stronger predictive capability for tSRE and TTP than single parameters or other multivariable models. Patients with greater reductions in uptake on scan2 versus scan1 were found to have improved prognosis. Specifically, patients in whom the difference between scan2 and scan1 was 1 SD lower (greater decline with therapy) saw a 75% decrease (HR, 4.14) in risk of tSRE ($P < 0.01$) and a decrease of 50% (HR, 1.98) in risk of progression ($P = 0.02$), suggesting that the combination of ^{18}F-FDG uptake measures from both scans identifies patients at risk for skeletal-related events or disease progression. Results were similar using SUL_{peak} in this model. Kaplan–Meier curves for the multivariable analysis are shown in Supplemental Figure 1.

Table 5 and Figure 2 show response by mPERCIST. Eleven patients had PD by mPERCIST, whereas 1 patient had CR, 6 patients had PR, and 6 had stable disease. Four patients were unevaluable, either because none of the lesions was above the liver SUL_{peak} threshold ($n = 3$) or there was liver disease present and an alternative aorta ROI was not available. Supplemental Table 7 details the tumor response parameters. Responding patients (mPERCIST CR+PR+ stable disease) ($n = 13$) had significant prolongation of tSRE, TTP, and a trend toward improved OS (not statistically significant) compared with nonresponders (PD). The median tSRE of patients in the response group was 47.6 mo (95% confidence interval [CI]: 29.7 to NA mo) compared with 4.6 mo (95% CI: 4.1 to NA mo) in patients with PD ($P = 0.007$). The median TTP of patients in response group was 14.1 mo (95% CI: 5.4 to NA mo) compared with 3.8 mo (95% CI: 3.5 to NA mo) in patients with PD ($P = 0.028$). Similarly, the median OS of patients in response group was 47.0 mo (95% CI: 23.7 to NA mo) compared with 25 mo (95% CI: 18.5 to NA mo) in patients with PD, but was not statistically significant ($P = 0.10$).

PERCIST have not been evaluated for ^{18}F-NaF PET, however, we note that in 8 patients who underwent both ^{18}F-FDG PET and ^{18}F-NaF PET scans with PD by ^{18}F-FDG PET mPERCIST, 5 of 8 (63%) were considered PD because of new ^{18}F-FDG–avid lesions, but only 3 of 8 (38%) had new lesions noted in their ^{18}F-NaF PET scans. No scans that were not considered PD by ^{18}F-FDG PET were considered PD by ^{18}F-NaF PET.

DISCUSSION

The ability to accurately detect metastases in breast and prostate cancers has improved significantly in recent years with hybrid

TABLE 2
Uptake Characteristics

Characteristic	Scan1	Scan2	Unit change (scan2 – scan1)	% change (scan2 – scan1)
A: ^{18}F-FDG SUV_{max} ($n = 28$)				
Index lesion	10.0 (3.0–31.3)	6.9 (2.4–16.9)	−2.87 (−20.7–4.1)	−16 (−83–117)
Up to 5 lesions	7.6 (2.7–20.2)	5.7 (2.1–13)	−1.7 (−16.9–3.0)	−14 (−84–65)
B: ^{18}F-FDG SUL_{peak} ($n = 28$)				
Index lesion	5.1 (1.2–14.3)	4.1 (1.2–12.3)	−1.0 (−11.8–7.0)	−3 (−83–133)
Up to 5 lesions	3.9 (1.0–11.5)	3.3 (1.0–10.7)	−0.58 (−9.6–6.4)	−2 (−85–147)
C: ^{18}F-NaF SUV_{max} ($n = 24$)				
Index lesion	34.37 (12.0–73.7)	31.11 (12.7–68.8)	−3.26 (−44.0–16.6)	−2.52 (−59.6–46.8)
Up to 5 lesions	27.77 (12.0–60.2)	24.47 (12.7–61.1)	−3.30 (−34.2–16.6)	−7.58 (−56.7–39.3)

A and B are mean (with range in parentheses) for ^{18}F-FDG SUV_{max} and SUL_{peak} uptake values and change in uptake for 28 patients completing 2 ^{18}F-FDG PET scans. C is mean (with range in parentheses) for ^{18}F-NaF SUV_{max} values and change in uptake for 24 patients completing 2 ^{18}F-NaF PET and 2 ^{18}F-FDG PET scans.

TABLE 3
Univariate Analysis of ^{18}F-FDG PET and ^{18}F-NaF PET Parameters and Clinical Endpoints

Parameter	tSRE				TTP				OS			
	HR	*P*	R^2	*C*	HR	*P*	R^2	*C*	HR	*P*	R^2	*C*
A: ^{18}F-FDG SUV_{max} ($n = 28$)												
Index lesion												
$SUV_{max}1$	1.38	0.159	0.060	0.631	1.09	0.679	0.006	0.507	1.28	0.196	0.052	0.580
$SUV_{max}2$	2.27	<0.001	0.304	0.787	1.36	0.130	0.072	0.584	1.12	0.642	0.008	0.528
Unit difference	1.18	0.576	0.012	0.653	1.07	0.710	0.005	0.578	0.81	0.290	0.036	0.528
% difference	1.12	0.579	0.010	0.688	0.94	0.682	0.006	0.403	0.71	0.112	0.098	0.547
Up to 5 lesions												
Unit difference	1.52	0.246	0.061	0.670	1.23	0.302	0.042	0.629	0.88	0.525	0.013	0.512
% difference	1.35	0.191	0.058	0.677	1.10	0.568	0.012	0.613	0.82	0.320	0.035	0.536
B: ^{18}F-FDG SUL_{peak} ($n = 28$)												
Index lesion												
$SUL_{peak}1$	1.18	0.447	0.019	0.589	1.03	0.855	0.001	0.496	1.26	0.215	0.049	0.566
$SUL_{peak}2$	2.41	<0.001	0.308	0.755	1.58	0.044	0.122	0.589	1.33	0.290	0.037	0.534
Up to 5 lesions												
Unit difference	2.21	0.038	0.165	0.684	1.40	0.155	0.080	0.626	0.999	0.999	0	0.493
C: ^{18}F-NaF SUV_{max} ($n = 24$)												
Index lesion												
$SUV_{max}1$	1.22	0.381	0.030	0.571	1.15	0.426	0.025	0.564	1.21	0.334	0.037	0.532
$SUV_{max}2$	1.16	0.440	0.023	0.528	1.38	0.138	0.077	0.582	1.00	0.986	0.000	0.424
Unit difference	0.943	0.827	0.002	0.547	1.01	0.946	0.0	0.48	0.77	0.212	0.056	0.587
% difference	0.874	0.647	0.008	0.547	0.94	0.8	0.003	0.538	0.70	0.169	0.072	0.591
Up to 5 lesions												
Unit difference	0.854	0.630	0.010	0.504	0.83	0.443	0.023	0.564	0.71	0.109	0.090	0.665
% difference	0.861	0.623	0.010	0.528	0.81	0.321	0.040	0.567	0.58	0.027	0.191	0.669

A and B are ^{18}F-FDG SUV_{max} and SUL_{peak} values and change in uptake for 28 patients with 2 ^{18}F-FDG PET scans. C is ^{18}F-NaF SUV_{max} and percentage change in uptake for 24 patients with 2 ^{18}F-NaF PET and 2 ^{18}F-FDG PET scans.

imaging methods. Nevertheless, no consensus has been reached on the best imaging modality for treatment response assessment of breast cancer bone metastases (*44*). We hypothesized that serial ^{18}F-FDG PET and ^{18}F-NaF PET would provide complementary measures of activity of breast cancer bone metastases and that each might predict response to therapy.

TABLE 4
Multivariable Analysis (^{18}F-FDG Only)

Parameter	tSRE				TTP				OS			
	HR	*P*	R^2	*C*	HR	*P*	R^2	*C*	HR	*P*	R^2	*C*
A: SUV_{max} ($n = 28$)												
$SUV_{max}1$ (index lesion)	3.66	4.0E−4	0.379	0.805	2.00	0.021	0.187	0.658	1.38	0.236	0.057	0.563
Unit difference (up to 5 lesions)	4.14	0.006			1.98	0.021			1.11	0.712		
B: SUL_{peak} ($n = 28$)												
$SUL_{peak}1$ (index lesion)	2.93	0.004	0.385	0.794	1.98	0.022	0.234	0.650	1.69	0.070	0.106	0.582
Unit difference (up to 5 lesions)	4.14	0.006			2.34	0.004			1.56	0.183		

A shows multivariable analysis using ^{18}F-FDG SUV_{max} uptake at scan1 plus unit difference in SUV_{max} for up to 5 lesions. B includes same variables, but for SUL_{peak}.

TABLE 5
Response by mPERCIST

Response	*n* = 24 (%)	tSRE (95% CI)	TTP (95% CI)	OS (95% CI)
Responders (CR+PR+ stable disease)	13 (54%)	47.6 mo (29.7–NA)	14.1 mo (5.4–NA)	47 mo (23.7–NA)
Nonresponders (PD)	11 (45%)	4.6 mo (4.1–NA)	3.8 mo (3.5–NA)	25 mo (18.5–NA)

Median and 95% CIs for each response measured for 24 patients.
NA = not available.

Our ^{18}F-FDG PET results were consistent with previously reported retrospective data for breast cancer (*26–29*) and similar to studies in castrate-resistant prostate cancer, which tends to have higher ^{18}F-FDG uptake than hormone-sensitive disease (*45*). Neither ^{18}F-NaF PET measures at scan1 or scan2 nor change in NaF SUV uptake over the course of treatment were predictive of tSRE or TTP. However, the percentage difference (but not the unit difference) of the average SUV_{max} of up to 5 lesions was associated with OS. The direction of the hazard ratio (HR) suggests that an increase in uptake was predictive, but the association does not persist when SUV uptake is corrected for normal bone uptake. This may be related to the flare effect, artifactual, or related to effects not specific to the metastases, as seen in a similar study in prostate cancer (*46*). Additional analyses evaluating performance of serial NaF by lesion type (lytic vs. sclerotic vs. mixed) also failed to demonstrate predictive value of NaF (Supplemental Table 6). The difference between our results for ^{18}F-NaF PET and the promising results in prostate cancer (*46–49*), particularly when quantitative assessment of NaF uptake is incorporated (*34*), may relate to biologic differences in breast cancer bone metastases. Breast cancer lesions, although phenotypically both blastic and lytic, tend to be more driven by primarily lytic molecular process compared with prostate cancer metastases (*50*). Our ^{18}F-NaF PET results are consistent with other studies showing confounding responses for breast cancer bone metastases by bone scanning and ^{18}F-NaF PET (*14,51*). Although useful as a mode of detection of osteoblastic bone lesions, our results do not support use of serial ^{18}F-NaF PET as a response measure or predictor of clinical outcomes in BD MBC.

There are several limitations to this study including small sample size (*n* = 28). We found a wide range of SUVs in bony lesions by both ^{18}F-FDG PET and ^{18}F-NaF PET, likely due to heterogeneity in lytic versus sclerotic lesions, which may be related to both underlying tumor biologic differences and prior therapy (*20,22,52*). Treatment while on the study incorporated standard endocrine agents or chemotherapy prescribed at physician discretion and the timing of PET posttherapy scanning was not uniform, influenced by clinical practice. Results of the multivariable analysis should be considered exploratory and parameters from the model validated in larger studies.

Some patients were imaged on different scanners, all in the same institution with similar patient preparation and where machine calibrations were done quarterly using the same calibration procedures and daily quality control to keep them as closely aligned as possible. Recent work demonstrated that ^{18}F-FDG PET scanner qualification and calibration can yield highly reproducible SUV measurements with a percentage test–retest difference in tumor SUV_{max} for bone of 7% and for soft tissue 10% (data not shown).

We found that mPERCIST criteria may be valuable to assess response to therapy and are associated with differences in clinical endpoints (*41,53*). Lower average ^{18}F-FDG uptake in bone versus soft-tissue metastases prompted our modification to include bone

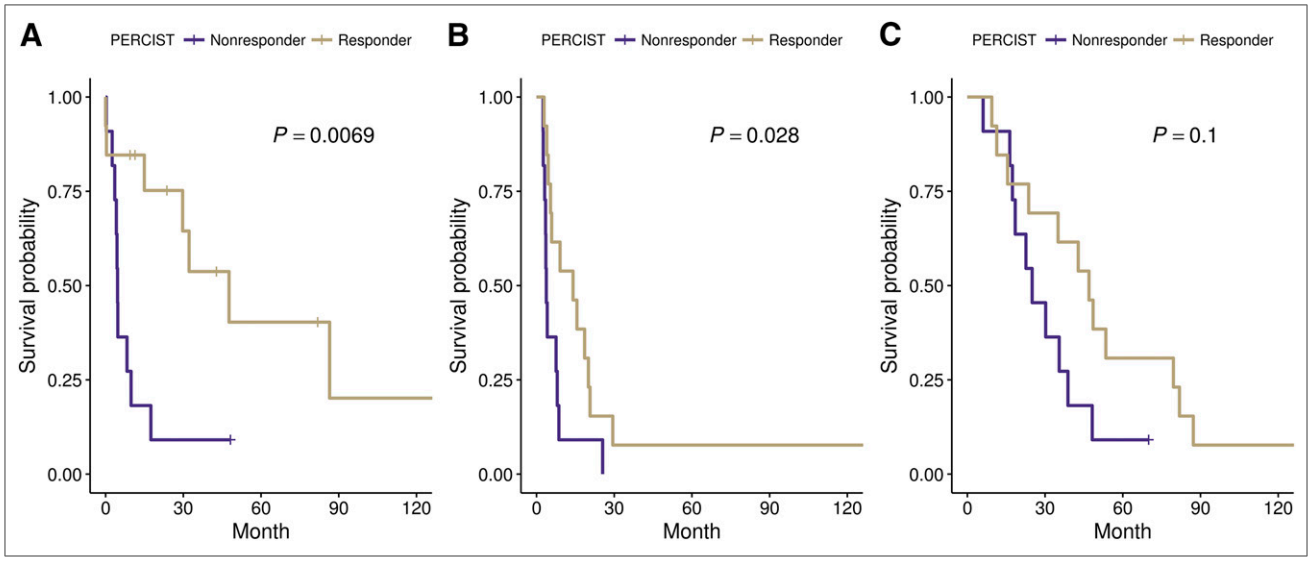

FIGURE 2. Kaplan–Meier plots for ^{18}F-FDG mPERCIST response criteria. Responders by mPERCIST (CR, PR, or stable disease) (*n* = 13) and nonresponders (*n* = 11). (A) tSRE. (B) TTP. (C) OS.

lesions with an SUL_{peak} greater than 1.5× the value of normal liver. We found that patients with metabolic response (CR, PR, and stable disease) experienced significant prolongation in tSRE (47.6 vs. 4.6 mo) and TTP (14.1 vs. 3.8 mo). ^{18}F-FDG PET uptake changes assessed by mPERCIST were strongly associated with clinical outcomes of interest. Our results support the use of ^{18}F-FDG PET and a modified PERCIST approach to monitor response to therapy in BD MBC and indicate a need for validation in larger prospective, multicenter trials.

CONCLUSION

This prospective study of serial and ^{18}F-FDG PET and ^{18}F-NaF PET in patients with BD MBC confirmed prior retrospective studies showing that ^{18}F-FDG uptake measures predict key clinical outcomes (tSRE and TTP) and supported the use mPERCIST. Our results do not support a clear role for serial ^{18}F-NaF PET in this patient population. These results endorse a larger prospective trial of ^{18}F-FDG PET/CT as a response endpoint for BD MBC and suggest that ^{18}F-FDG PET/CT could be used as a response endpoint that would increase access of this patient population to clinical trials and promising new therapies.

DISCLOSURE

This study was sponsored by R01CA124573, Komen SAC130060, P30CA015704, and SFI 11/PI/1027. No other potential conflict of interest relevant to this article was reported.

ACKNOWLEDGMENTS

We thank the patients who participated in the study. We also thank Finbarr O'Sullivan, Lisa Dunnwald, Erin Schubert, William Barlow, Robert Doot, and Larry MacDonald and all of the radiochemistry staff, technologists, physicists, and physicians who helped with this study.

REFERENCES

1. Jung SY, Rosenzweig M, Sereika SM, Linkov F, Brufsky A, Weissfeld JL. Factors associated with mortality after breast cancer metastasis. *Cancer Causes Control.* 2012;23:103–112.
2. Manders K, van de Poll-Franse LV, Creemers GJ, et al. Clinical management of women with metastatic breast cancer: a descriptive study according to age group. *BMC Cancer.* 2006;6:179–186.
3. Nielsen OS, Munro AJ, Tannock IF. Bone metastases: pathophysiology and management policy. *J Clin Oncol.* 1991;9:509–524.
4. Plunkett TA, Smith P, Rubens RD. Risk of complications from bone metastases in breast cancer. implications for management. *Eur J Cancer.* 2000;36:476–482.
5. Ahn SG, Lee HM, Cho SH, et al. Prognostic factors for patients with bone-only metastasis in breast cancer. *Yonsei Med J.* 2013;54:1168–1177.
6. Cetin K, Christiansen CF, Svaerke C, Jacobsen JB, Sorensen HT. Survival in patients with breast cancer with bone metastasis: a Danish population-based cohort study on the prognostic impact of initial stage of disease at breast cancer diagnosis and length of the bone metastasis-free interval. *BMJ Open.* 2015;5:e007702.
7. Dawood S, Broglio K, Ensor J, Hortobagyi GN, Giordano SH. Survival differences among women with de novo stage IV and relapsed breast cancer. *Ann Oncol.* 2010;21:2169–2174.
8. Harries M, Taylor A, Holmberg L, et al. Incidence of bone metastases and survival after a diagnosis of bone metastases in breast cancer patients. *Cancer Epidemiol.* 2014;38:427–434.
9. Puente J, Lopez-Tarruella S, Ruiz A, et al. Practical prognostic index for patients with metastatic recurrent breast cancer: retrospective analysis of 2,322 patients from the GEICAM Spanish El Alamo Register. *Breast Cancer Res Treat.* 2010; 122:591–600.
10. Solomayer EF, Diel IJ, Meyberg GC, Gollan C, Bastert G. Metastatic breast cancer: clinical course, prognosis and therapy related to the first site of metastasis. *Breast Cancer Res Treat.* 2000;59:271–278.
11. Cook GJ, Azad GK, Goh V. Imaging bone metastases in breast cancer: staging and response assessment. *J Nucl Med.* 2016;57(suppl 1):27S–33S.
12. Hamaoka T, Madewell JE, Podoloff DA, Hortobagyi GN, Ueno NT. Bone imaging in metastatic breast cancer. *J Clin Oncol.* 2004;22:2942–2953.
13. Maffioli L, Florimonte L, Pagani L, Butti I, Roca I. Current role of bone scan with phosphonates in the follow-up of breast cancer. *Eur J Nucl Med Mol Imaging.* 2004;31(suppl 1):S143–S148.
14. Schneider JA, Divgi CR, Scott AM, et al. Flare on bone scintigraphy following Taxol chemotherapy for metastatic breast cancer. *J Nucl Med.* 1994;35:1748–1752.
15. Vogel CL, Schoenfelder J, Shemano I, Hayes DF, Gams RA. Worsening bone scan in the evaluation of antitumor response during hormonal therapy of breast cancer. *J Clin Oncol.* 1995;13:1123–1128.
16. Kimura M, Tominaga T. Outstanding problems with response evaluation criteria in solid tumors (RECIST) in breast cancer. *Breast Cancer.* 2002;9:153–159.
17. Gibbs J, Partridge S, Lobo C, Hylton N. Value of RECIST (unidimensional), WHO (bidimensional) and volumetric measures of breast tumor response on MRI for predicting recurrence free survival in patients undergoing preoperative chemotherapy. Paper presented at: International Society of Magnetic Resonance in Medicine 13th Scientific Meeting; May 7–13, 2005; Miami, FL.
18. Eisenhauer EA, Therasse P, Bogaerts J, et al. New response evaluation criteria in solid tumours: revised RECIST guideline (version 1.1). *Eur J Cancer.* 2009;45: 228–247.
19. Wei S, Li Y, Siegal GP, Hameed O. Breast carcinomas with isolated bone metastases have different hormone receptor expression profiles than those with metastases to other sites or multiple organs. *Ann Diagn Pathol.* 2011;15:79–83.
20. Cook GJ, Fogelman I. The role of positron emission tomography in the management of bone metastases. *Cancer.* 2000;88:2927–2933.
21. Cook GJ, Fogelman I. Detection of bone metastases in cancer patients by ^{18}F-fluoride and ^{18}F-fluorodeoxyglucose positron emission tomography. *Q J Nucl Med.* 2001;45:47–52.
22. Fogelman I, Cook G, Israel O, Van der Wall H. Positron emission tomography and bone metastases. *Semin Nucl Med.* 2005;35:135–142.
23. Biersack HJ, Bender H, Palmedo H. FDG-PET in monitoring therapy of breast cancer. *Eur J Nucl Med Mol Imaging.* 2004;31(suppl 1):S112–S117.
24. D'Amico A, Kowalska T. Paradoxal metabolic flare detected by ^{18}F-fluorodeoxyglucose positron emission tomography in a patient with metastatic breast cancer treated with aromatase inhibitor and biphosphonate. *Indian J Nucl Med.* 2014;29:34–37.
25. Mortimer JE, Dehdashti F, Siegel BA, Trinkaus K, Katzenellenbogen JA, Welch MJ. Metabolic flare: indicator of hormone responsiveness in advanced breast cancer. *J Clin Oncol.* 2001;19:2797–2803.
26. Stafford SE, Gralow JR, Schubert EK, et al. Use of serial FDG PET to measure the response of bone-dominant breast cancer to therapy. *Acad Radiol.* 2002;9:913–921.
27. Specht JM, Tam SL, Kurland BF, et al. Serial 2-[^{18}F] fluoro-2-deoxy-D-glucose positron emission tomography (FDG-PET) to monitor treatment of bone-dominant metastatic breast cancer predicts time to progression (TTP). *Breast Cancer Res Treat.* 2007;105:87–94.
28. Tateishi U, Gamez C, Dawood S, Yeung HW, Cristofanilli M, Macapinlac HA. Bone metastases in patients with metastatic breast cancer: morphologic and metabolic monitoring of response to systemic therapy with integrated PET/CT. *Radiology.* 2008;247:189–196.
29. De Giorgi U, Mego M, Rohren EM, et al. ^{18}F-FDG PET/CT findings and circulating tumor cell counts in the monitoring of systemic therapies for bone metastases from breast cancer. *J Nucl Med.* 2010;51:1213–1218.
30. Abikhzer G, Srour S, Fried G, et al. Prospective comparison of whole-body bone SPECT and sodium ^{18}F-fluoride PET in the detection of bone metastases from breast cancer. *Nucl Med Commun.* 2016;37:1160–1168.
31. Brenner W, Vernon C, Muzi M, et al. Comparison of different quantitative approaches to ^{18}F-fluoride PET scans. *J Nucl Med.* 2004;45:1493–1500.
32. Yildiz M, Oral B, Bozkurt M, Cobaner A. Relationship between bone scintigraphy and tumor markers in patients with breast cancer. *Ann Nucl Med.* 2004;18:501–505.
33. Yoon SH, Kim KS, Kang SY, et al. Usefulness of ^{18}F-fluoride PET/CT in breast cancer patients with osteosclerotic bone metastases. *Nucl Med Mol Imaging.* 2013;47:27–35.
34. Harmon SA, Perk T, Lin C, et al. Quantitative assessment of early [^{18}F]sodium fluoride positron emission tomography/computed tomography response to treatment in men with metastatic prostate cancer to bone. *J Clin Oncol.* 2017;35:2829–2837.
35. Hamacher K, Coenen HH, Stocklin G. Efficient stereospecific synthesis of no-carrier-added 2-[^{18}F]-fluoro-2-deoxy-D-glucose using aminopolyether supported nucleophilic substitution. *J Nucl Med.* 1986;27:235–238.

36. Schlyer DJ, Bastos MA, Alexoff D, Wolf AP. Separation of [^{18}F]fluoride from [^{18}O]water using anion exchange resin. *Int J Rad Appl Instrum [A].* 1990;41: 531–533.
37. Shankar LK, Hoffman JM, Bacharach S, et al. Consensus recommendations for the use of ^{18}F-FDG PET as an indicator of therapeutic response in patients in National Cancer Institute Trials. *J Nucl Med.* 2006;47:1059–1066.
38. Lockhart CM, MacDonald LR, Alessio AM, McDougald WA, Doot RK, Kinahan PE. Quantifying and reducing the effect of calibration error on variability of PET/CT standardized uptake value measurements. *J Nucl Med.* 2011;52: 218–224.
39. Byrd D, Christopfel R, Arabasz G, et al. Measuring temporal stability of positron emission tomography standardized uptake value bias using long-lived sources in a multicenter network. *J Med Imaging (Bellingham).* 2018;5:011016.
40. Peterson L, Kurland BF, Shields AF, et al. Reproducibility of FDG SUVmax for metastatic breast cancer lesions in the same or different PET/CT scanners in a local network [abstract]. *J Nucl Med.* 2014;55(suppl 1):1505.
41. Wahl RL, Jacene H, Kasamon Y, Lodge MA. From RECIST to PERCIST: evolving considerations for PET response criteria in solid tumors. *J Nucl Med.* 2009;50(suppl 1):122S–150S.
42. O JH, Lodge MA, Wahl RL. Practical PERCIST: a simplified guide to PET response criteria in solid tumors 1.0. *Radiology.* 2016;280:576–584.
43. Harrell FE. Cox proportional hazards regression model. In: Harrell FE, ed. *Regression Modeling Strategies. Springer Series in Statistics*. New York, NY: Springer; 2001:466.
44. Azad GK, Taylor B, Rubello D, Colletti PM, Goh V, Cook GJ. Molecular and functional imaging of bone metastases in breast and prostate cancers: an overview. *Clin Nucl Med.* 2016;41:e44–e50.
45. Morris MJ, Akhurst T, Larson SM, et al. Fluorodeoxyglucose positron emission tomography as an outcome measure for castrate metastatic prostate cancer treated with antimicrotubule chemotherapy. *Clin Cancer Res.* 2005;11:3210–3216.
46. Yu EY, Duan F, Muzi M, et al. Castration-resistant prostate cancer bone metastasis response measured by ^{18}F-fluoride PET after treatment with dasatinib and correlation with progression-free survival: results from American College of Radiology Imaging Network 6687. *J Nucl Med.* 2015;56:354–360.
47. Apolo AB, Lindenberg L, Shih JH, et al. Prospective study evaluating Na18F PET/CT in predicting clinical outcomes and survival in advanced prostate cancer. *J Nucl Med.* 2016;57:886–892.
48. Gareen IF, Hillner BE, Hanna L, et al. Hospice admission and survival after ^{18}F-fluoride PET performed for evaluation of osseous metastatic disease in the national oncologic PET registry. *J Nucl Med.* 2018;59:427–433.
49. Hillner BE, Siegel BA, Hanna L, Duan F, Quinn B, Shields AF. ^{18}F-fluoride PET used for treatment monitoring of systemic cancer therapy: results from the National Oncologic PET Registry. *J Nucl Med.* 2015;56:222–228.
50. Roodman GD. Mechanisms of bone metastasis. *N Engl J Med.* 2004;350:1655–1664.
51. Wade AA, Scott JA, Kuter I, Fischman AJ. Flare response in ^{18}F-fluoride ion PET bone scanning. *AJR.* 2006;186:1783–1786.
52. Cook GJ, Lodge MA, Marsden PK, Dynes A, Fogelman I. Non-invasive assessment of skeletal kinetics using fluorine-18 fluoride positron emission tomography: evaluation of image and population-derived arterial input functions. *Eur J Nucl Med.* 1999;26:1424–1429.
53. O JH, Leal J, Stearns V, Wahl R. Assessing PERCIST 1.0 non-measurable (low FDG uptake) lesions in patients with breast cancer does not diminish the predictive value of FDG PET. *J Nucl Med.* 2013;54(suppl 2):73.